ligands, and the propylene bridge in PnAO complexes imposes no significant constraint on these complexes.

An X-ray diffraction study of $[Co((AO)_2\text{-}H)Cl_2]$[2] has revealed an O---O distance of 2.422 (3) Å. With that same bidentate α-amine oxime ligand occupying a square plane in $[Rh((AO)_2\text{-}H)Cl_2]$, an O---O distance of 2.459 (2) Å is observed. In $[Rh(PnAO\text{-}H)Cl_2]$, the O---O distance is 2.474 (7) Å, which is longer than 2.432 (3) Å observed in the $[Co(PnAO\text{-}H)(NO_2)_2]$ complex.[3] The above results reveal the effect of the size of the metal ion on the hydrogen bond. The elongation of 0.037–0.042 Å in the O---O distance on going from Co(III) to Rh(III) can be associated with the larger size of Rh(III). The increase in the M–N–O angle by about 2° on going from Rh to Co further indicates the different effects of the two metals and suggests a repulsive interaction of the oxygen atoms in the cobalt complexes. In nickel(II) complexes,[6,8] this angle is also approximately 2° larger than in the corresponding Pd(II)[9] and Pt(II)[7] complexes.

The infrared spectra have no unusual features except the broad band at 1785 (5) cm^{-1} for each compound that is associated with the short O---H---O hydrogen bond.

The proton NMR spectrum of $[Rh(PnAO\text{-}H)Cl_2]$ has methyl proton resonances (2:1 ratio) at 1.40 and 2.05 ppm relative to Me_4Si. The former is a bit broader, which is attributed to the slight difference in environment of the two methyl groups on a chelate-ring sp^3 carbon (C(7) and C(9) compared with C(8) and C(10)). The methylene protons are apparently strongly coupled and result in a broad multiplet at 3.05 ppm while the amine hydrogens give a broad resonance at 4.80 ppm. The O--H---O hydrogen-bond resonance appears at 18.9 ppm. For $[Rh((AO)_2\text{-}H)Cl_2]$, the methyl resonances (2:1 ratio) appear at 1.35 and 2.00 ppm while the amine hydrogen resonance appears at 5.2 ppm and the O---H---O hydrogen-bond resonance appears at 19.3 ppm. The slight shift in the O---H---O resonance is in the downfield direction as the O---O distance shortens from 2.474 (7) Å in the PnAO complex to 2.459 (2) Å in the AO complex. Additional studies of this correlation are under way.

The present and earlier comparison of AO and PnAO complexes of Rh(III) and other metal ions (Table VII) indicates that introduction of a propylene bridge opposite the hydrogen bond with metals of this approximate size, or smaller, imposes no significant constraint on the hydrogen bond. When they are compared with the corresponding Co(III) complexes,[2,3] however, significant lengthening of the hydrogen bond is found with the larger Rh(III) ion.

Acknowledgment. Financial support from the National Science Foundation (Grant CHE81-06795) is gratefully acknowledged.

Registry No. $[Rh(PnAO\text{-}H)Cl_2]$, 88245-18-5; $[Rh((AO)_2\text{-}H)Cl_2]$, 88245-19-6.

Supplementary Material Available: Listings of observed and calculated structure factors, temperature factor expressions, and hydrogen positional parameters for both complexes, intermolecular distances in $[Rh(PnAO\text{-}H)Cl_2]$ (Table IV), and stereoscopic views of both unit cells (Figures 3 and 4) (35 pages). Ordering information is given on any current masthead page.

Contribution from the Department of Physics, Nuclear Research Center "Demokritos", Athens, Greece

Structure and Magnetic Behavior of Iron(III) Dithiocarbamate Complexes Exhibiting $S = |^1/_2\rangle \rightleftarrows S = |^5/_2\rangle$ Thermal Equilibrium. Study of the Tris(*N*-methyl-*N*-*n*-butyldithiocarbamato)iron Homologue

A. TERZIS,* S. FILIPPAKIS, D. MENTZAFOS, V. PETROULEAS, and ANGELOS MALLIARIS*

Received April 26, 1983

The molecular and crystal structures of the nonsolvated title complex have been determined at 300 K and its magnetic behavior has been studied by combined magnetic susceptibility measurement and Mössbauer spectroscopy in the temperature range between 300 and 77 K. The complex exhibits strong high–low-spin thermal equilibrium with a predominant contribution from the $S = |^5/_2\rangle$ state at high temperature and a drastic shift toward the $S = |^1/_2\rangle$ state at the low-temperature limit. Crystals are hexagonal $P3_1/c$, with $a = 14.970$ Å, $c = 14.390$ Å, $V = 2792.8$ Å^3, and $Z = 4$, and contain two independent complexes A and B, both sitting on the crystallographic threefold axis. The iron–sulfur bond distance $\langle Fe\text{–}S\rangle = 2.367$ Å and the mean room-temperature effective magnetic moment $\mu_{eff}(300\ K) = 4.72\ \mu_B$ are in good agreement with the corresponding values reported for other homologues also exhibiting high–low-spin thermal equilibrium.

Introduction

Complexes of octahedrally coordinated ferric ions can exist in two distinct spin states depending on the strength of the ligand field. Thus, in the presence of strong fields of O_h symmetry the term $^2T_{2g}$ (t_{2g}^5) lies lowest in energy and the iron ion is in the $S = {}^1/_2$ "low" spin state. The room-temperature value of the effective magnetic moment is in this case close to 2.0 μ_B, somewhat higher than the spin-only value $\mu_{eff} = 1.73\ \mu_B$, due to the small contribution from the non-zero value of the orbital angular momentum in the t_{2g}^5 configuration.[1,2] Under weak ligand fields of O_h symmetry, on the other hand, the $^6A_{1g}$ ($t_{2g}^3e_g^2$) term becomes the ground state of the system with $S = {}^5/_2$ "high" spin and observed moments close to the spin-only value of 5.9 μ_B. Deviations from pure high- or low-spin behavior can arise in these and other complexes when the ligand field strength is comparable with the mean electron pairing energy of the d^5 configuration. In this case thermal equilibrium can be established between the two possible ground states $^2T_{2g}$ and $^6A_{1g}$, resulting in variation of the magnetic moments between the limiting values of 2.0 and 5.9 μ_B. Tris(*N*,*N*-dialkyldithiocarbamato)iron(III) complexes constitute a typical class of molecules exhibiting high–low-spin thermal equilibrium. Magnetic susceptibility measurements, Mössbauer spectral behavior, and NMR shifts of numerous examples of these compounds have been successfully interpreted in terms of the $S = |^1/_2\rangle \rightleftarrows S = |^5/_2\rangle$ thermal equilibrium.[2-7] Failure to observe simultaneous population of both

(1) Figgis, B. N. *Trans. Faraday Soc.* **1961**, *57*, 198, 204.
(2) White, A. H.; Roper, R.; Kokot, E.; Waterman, H.; Martin, R. L. *Aust. J. Chem.* **1964**, *17*, 204.
(3) Ewald, A. H.; Martin, R. L.; Ross, I. G.; White, A. H. *Proc. R. Soc. London, Ser. A* **1964**, *280*, 235.

0020-1669/84/1323-0334$01.50/0

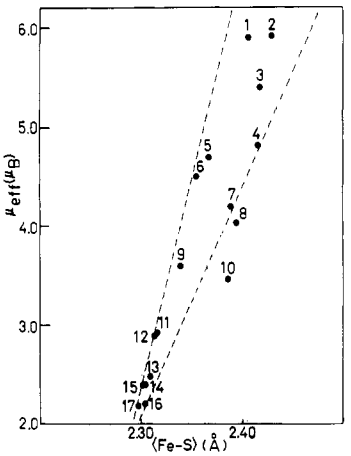

Figure 1. Plot of μ_{eff} (μ_B) vs. ⟨Fe–S⟩ distance (Å) for ferric tris(R-dithiocarbamato) complexes. R groups are as follows: (1) pyrrolidinyl;[10] (2) morpholyl (CH_2Cl_2 solvate);[25] (3) *n*-butyl;[23] (4) methyl (400 K);[24] (5) methyl-*n*-butyl (this work); (6) ethyl;[11] (7) ethoxy;[25] (8) methyl;[26] (9) *n*-butyl (C_6H_6 solvate);[27] (10) benzyl;[25] (11) morpholyl ($2C_6H_6$ solvate);[26] (12) methylphenyl;[10] (13) benzyl (150 K);[25] (14) methyl (150 K);[26] (15) ethoxy (150 K);[26] (16) pyrrolyl ($0.5C_6H_6$ solvate);[28] (17) ethyl (79 K).[11] Dashed lines indicate the approximate region in the μ_{eff}/vs. ⟨Fe–S⟩ plot for most of the iron(III) $(dtc)_3$ complexes.

the $^2T_{2g}$ and $^6A_{1g}$ states by Mössbauer and NMR spectroscopy has been attributed mainly to high–low-spin crossover periods shorter than the iron Mössbauer and proton NMR time scales ($\sim 10^7$ Hz), although alternative explanations have also been proposed.[8,9]

X-ray studies have shown that the stereochemistry of the FeS_6 core in the six-coordinate ferric dithiocarbamate complexes is that of a trigonally distorted octahedron rather than pure octahedral.[10,11] Moreover, it has been established that several of these complexes crystallize with solvated solvent molecules occupying crystallographic positions in the unit cell.[12-15] The effect of the solvated solvent on the magnetic behavior of the ferric ion has been clearly demonstrated in the case of the morpholyl derivative, which was found to have μ_{eff} = 2.92 μ_B when benzene solvated and μ_{eff} = 5.92 μ_B when dichloromethane solvated.[16]

Since structural data are available only for some iron(III) dithiocarbamate complexes (Figure 1), it seems interesing to study the structure of other homologues of this series in relation to their magnetic properties. In the present communication we report the molecular and crystal structure of nonsolvated tris(*N*-methyl-*N*-*n*-butyldithiocarbamato)iron(III) at 300 K as well as its magnetic behavior between 300 and 77 K.

Experimental Section

Tris(*N*-methyl-*N*-*n*-butyldithiocarbamato)iron (hereafter denoted $(mebudtc)_3Fe$) was prepared by stirring freshly precipitated ferric hydroxide with equimolar amounts of methyl-*n*-butylamine and carbon disulfide dissolved in absolute ethanol.[17] The precipitate was washed with ethanol and dried under vacuum for several hours at 100 °C to remove all traces of alcohol. It was then recrystallized from purified benzene/hexane under inert atmosphere in the dark to prevent photochemical reactions that lead to formation of five-coordinate complexes.[18] Well-developed hexagonal crystals were obtained in this way, while it was impossible to grow good crystals from other solvents such as $CHCl_3$, CH_2Cl_2, C_6H_{12}, CH_2Cl_2/C_6H_{12}, etc. The purity of the product and the absence of solvated benzene molecules was confirmed by C, H, N elemental analysis and IR spectroscopy. Magnetic susceptibility was measured on the PAR 155 vibrating-sample magnetometer using polycrystalline material, while for the Mössbauer spectra a ^{57}Co in Rh source was employed in conjunction with a linear drive.

Table I. Summary of Crystal and Intensity Collection Data

compd	$Fe(mebudtc)_3$
formula	$C_{18}H_{36}N_3S_6Fe$
fw	542.8
a, Å	14.970 (5)
c, Å	14.390 (3)
V, Å^3	2792.8
Z	4
D_{calcd}, g/cm^3	1.290
D_{measd}, g/cm^3	1.27
space group	$P3_1/c$
radiation	Mo Kα (0.71069 Å), Zr filtered
μ, cm^{-1}	9.6
scan speed, deg in 2θ/min	variable between 1 and 10
scan range, deg	0.8 below $K\alpha_1$ to 0.8 above $K\alpha_2$
bkgd counting, s	0.25 of scan time
2θ limit, deg	46
data form	hkl and $-h,-k,l$ with $h \leq k$
data collected/unique data	1462/1233
data used	1098 with $I > 2.5\sigma(I)$

Crystal Data. Preliminary oscillation and Weissenberg photographs indicated diffraction symmetry of $\bar{3}m$ and the systematic absence ($hh2hl$, $l = 2n + 1$) showed that the space group is either $P3_1/c$ or $P\bar{3}_1/c$. The cell parameters (Table I) were calculated by least-squares refinement of the setting angles of 14 automatically centered reflections ($24° < 2\theta < 25°$).

Collection and Reduction of Intensity Data. The crystal used for data collection was cut from a long hexagonal rod perpendicular to its *c* direction. It was a hexagonal prism of height 0.4 mm and a cross section diagonal of 0.25 mm. The crystal was mounted along its *c* direction on a $P2_1$ Syntex automatic diffractometer with Zr-filtered Mo Kα radiation. The intensities of 3 standard reflections monitored after every 67 reflections showed a 7% decrease during data collection, and a correction for this was applied during data reduction. The data were reduced with the Syntex XTL programs.[19] The integrated intensity was calculated as $I = (Ns - (ts/tB)(B1 + B2))(SR)$ and the standard deviations as $\sigma(I) = (SR)(Ns + (ts/tB)^2(B1 + B2))^{1/2}$, where Ns is the total scan count, B1 and B2 are the two background counts, ts and tB are the scan and total background time, respectively, and SR is the scan rate. Lorentz and polarization but no absorption corrections (μ = 9.58 cm^{-1}) were applied.

Solution and Refinement of the Structure. The *E* distribution strongly indicated that the space group is noncentrosymmetric. The origin-removed Patterson map showed Fe positions at the origin and at $^2/_3$, $^1/_3$, 0.3. The structure was solved in $P3_1/c$, and all non-hydrogen atom positions were located with the DIRDIF program.[19] Refinement was carried out by blocked full-matrix least-squares calculation in which $\sum w\Delta^2$ was minimized. Each of the two blocks contained one of the two independent Fe–thiocarbamato units. The weight for each reflection was initially unity and in the final cycles given by $w = (\sigma(F_o)^2 + cF_o^2)^{-1}$, where $c = 0.001$ was chosen such that the average values for $w\Delta^2$ for ranges of increasing F_o were almost constant. Isotropic refinement converged to an R ($=\sum||F_o| - |F_c||/\sum|F_o|$) of 0.116 and anisotropic refinement to R = 0.051. At this point the positions of

(4) Golding, R. M.; Whitfield, H. J. *Trans. Faraday Soc.* **1966**, *62*, 1713.
(5) Rickards, R.; Johnson, C. E.; Hill, H. A. D. *J. Chem. Phys.* **1968**, *48*, 5231.
(6) Wickman, H. H.; Wagner, C. F. *J. Chem. Phys.* **1969**, *51*, 435.
(7) Golding, R. M.; Tennant, W. C.; Bailey, J. P. M.; Hudson, A. *J. Chem. Phys.* **1968**, *48*, 764.
(8) Merrithew, P. B.; Rasmussen, P. G. *Inorg. Chem.* **1972**, *11*, 325.
(9) (a) Harris, G. *Theor. Chim. Acta* **1966**, *5*, 379. (b) Harris, G. *Ibid.* **1968**, *10*, 119.
(10) Healy, P. C.; White, A. H. *J. Chem. Soc., Dalton Trans.* **1972**, 1163.
(11) Leipoldt, J. G.; Coppens, P. *Inorg. Chem.* **1973**, *12*, 2269.
(12) Healy, P. C.; Sinn, E. *Inorg. Chem.* **1975**, *14*, 109.
(13) Butcher, R. J.; Sinn, E. *J. Am. Chem. Soc.* **1976**, *98*, 2440, 5139.
(14) Sinn, E. *Inorg. Chem.* **1976**, *15*, 369.
(15) Cuckauskas, E. J.; Deaver, B. S.; Sinn, E. *J. Chem. Phys.* **1977**, *67*, 1257.
(16) Malliaris, A.; Papaefthimious, V. *Inorg. Chem.* **1982**, *21*, 770.
(17) Golding, R. M.; Healy, P. C.; Neuman, P. W. G.; Sinn, E.; White, A. H. *Inorg. Chem.* **1972**, *11*, 2435.
(18) Miessler, G. L.; Zoebisch, E.; Pignolet, L. H. *Inorg. Chem.* **1978**, *17*, 3636.
(19) Computer programs used: SYNTEX XTL (data reduction); P. T. Beurskens' DIRDIF (phase extension); G. Sheldrick's SHELX-76 (Fourier least-squares refinement); C. K. Johnson's ORTEP (drawings).
(20) Epstein, L. M.; Straub, D. K. *Inorg. Chem.* **1969**, *8*, 784.

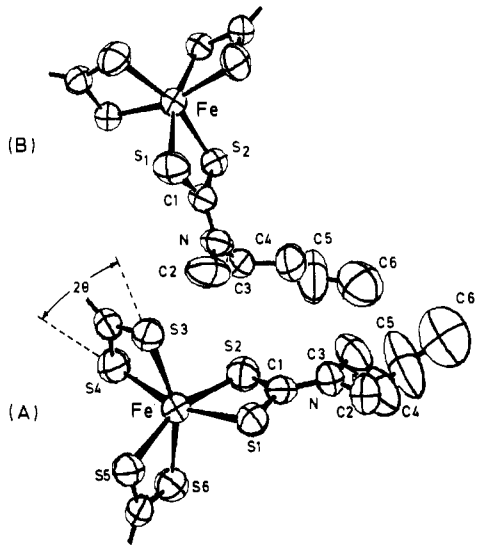

Figure 2. Drawings of complexes A and B viewed along the threefold axis. The thermal ellipsoids of the atoms are scaled to include 50% probability. H atoms are not shown. 2θ is the projection of the "bite" angle on the plane S1S3S5.

Table II. Positional ($\times 10^4$) Parameters of the Non-Hydrogen Atoms (Esd's in Parentheses)

	x	y	z
	Complex A		
Fe	0	0	0
S1	−240 (1)	1203 (2)	−937 (2)
S2	692 (2)	1573 (2)	869 (2)
C1	357 (5)	2055 (5)	−52 (6)
N	556 (5)	3032 (5)	−105 (5)
C2	256 (8)	3425 (7)	−921 (6)
C3	1090 (8)	3779 (6)	631 (7)
C4	320 (10)	3886 (9)	1217 (8)
C5	860 (10)	4751 (9)	1970 (10)
C6	1490 (10)	5733 (10)	1678 (10)
	Complex B		
Fe	6667	3333	3114 (1)
S1	5124 (2)	2518 (2)	2244 (2)
S2	5450 (1)	3514 (1)	4002 (1)
C1	4581 (5)	2838 (5)	3140 (5)
N	3602 (4)	2609 (5)	3180 (5)
C2	2899 (7)	2065 (9)	2395 (6)
C3	3199 (6)	2885 (6)	3948 (7)
C4	3184 (8)	3860 (8)	3847 (7)
C5	2920 (10)	4230 (9)	4740 (10)
C6	2760 (10)	5090 (10)	4630 (10)

the hydrogen atoms were calculated for a tetrahedral environment around carbon atoms and a C–H distance of 1.08 Å. These were refined as a rigid moiety (isotropic hydrogens riding on anisotropic carbons). The C3 and C4 carbons were set up as methyl groups that were refined as rigid bodies. The C11 and C12 hydrogen atoms were not included because of the high thermal motion of these carbon atoms. In general there was very high thermal motion in the two butyl chains (Figure 2), and this probably accounts for the very bad C–C distances. In the last two cycles of refinement an empirical isotropic extinction parameter was included, which led to the final values of $R = 0.0418$ and $R_w = [\sum w(|F_o| - |F_c|)^2/\sum w|F_o|^2]^{1/2} = 0.0581$ for 1098 reflections having $I > 2.5\sigma(I)$. During the last cycle of refinement the largest shift in any parameter was 0.2 times its estimated standard deviation. A final difference Fourier synthesis showed no peak greater than 0.35 e/Å^3. The final positional coordinates appear in Table II.

Results and Discussion

The unit cell contains the independent $(mebudtc)_3Fe$ monomolecular complexes A and B, both located on threefold crystallographic axes parallel to c. The fact that the two independent complexes occupy positions on threefold crystallographic axes imposes a molecular symmetry that appears to be the highest ever reported for this type of molecule.

Table III. Interatomic Distances (Å) and Angles (deg) of the Non-Hydrogen Atoms in Complexes A and B (Esd's in Parentheses)

	distances			angles	
	A	B		A	B
Fe–S1	2.416 (3)	2.360 (2)	S1–Fe–S2	73.2 (1)	74.6 (1)
Fe–S2	2.397 (3)	2.349 (2)	S1–Fe–S4	158.8 (1)	162.1 (2)
S1–C1	1.705 (8)	1.716 (9)	S1–Fe–S3	91.9 (1)	93.2 (1)
S2–C1	1.701 (9)	1.715 (7)	S2–Fe–S4	95.2 (1)	94.5 (1)
C1–N	1.34 (1)	1.33 (1)	S1–C1–S2	114.9 (5)	112.5 (4)
N–C2	1.48 (1)	1.48 (1)	S1–C1–N	121.4 (7)	125.2 (6)
N–C3	1.46 (1)	1.42 (1)	S2–C1–N	123.7 (6)	122.3 (6)
C3–C4	1.51 (2)	1.48 (2)	C1–N–C2	122.2 (7)	119.8 (8)
C4–C5	1.57 (2)	1.53 (2)	C1–N–C3	122.3 (8)	122.3 (6)
C5–C6	1.36 (2)	1.43 (3)	C2–N–C3	115.5 (8)	117.8 (7)
S1···S2	2.870 (4)	2.853 (3)	N–C3–C4	109.4 (8)	115.5 (8)
S1···S3	3.473 (4)	3.413 (4)	C3–C4–C5	111 (1)	114 (1)
S2···S4	3.541 (5)	3.465 (4)	C4–C5–C6	118 (1)	115 (1)

Molecular Structure. The interatomic distances and bond angles are tabulated in Table III for A and B complexes, and the numbering system of the atoms is shown in Figure 2. There are some significant and nontrivial structural differences in the FeS_6 core of the two complexes, whereas differences in the *n*-butyl group of the ligands must be attributed to the anomalously large thermal parameters at room temperature, probably indicating the presence of disorder in the butyl chain. Attempts to resolve this disorder failed. Similar disorders have been noticed for other dithiocarbamato complexes with even shorter alkyl groups.[12]

The symmetry of the FeS_6 core is that of a trigonally distorted octahedron, the degree of distortion being described by the angle $2\theta = 35.0°$ for A and 37.7° for B complexes (Figure 2). This angle measures the relative rotation between the upper and lower triangles S1S3S5 and S2S4S6 with respect to the threefold axis and it is equal to 60° for an octahedron and 0° for a trigonal prism. Typical values of this twist angle vary between 33 and 40° for all dithiocarbamates. Due to the threefold axis there are only two different Fe–S distances in each complex, Fe–S1 and Fe–S2. Their mean values are 2.406 and 2.327 Å for A and B, respectively. All four types of S–Fe–S angles, i.e. S1–Fe–S2 ("bite" angle), S1–Fe–S3, S2–Fe–S4, and S1–Fe–S4, have magnitudes (Table III) indicative of a distorted octahedron (for octahedral geometry the first three angles are qual to 90° and the fourth equal to 180°) but well within the limiting magnitudes known from other homologues.

The well-known conjugation of the S_2CN system in the dtc complexes is here also confirmed by the planarity of this fragment, but in the present case the same plane includes the central metal ion and the carbon atom of the methyl group as well as the first carbon of the *n*-butyl chain. The distance (Å) of these atoms from the best least-squares plane are as follows: for complex A, Fe (−0.04), S1 (0.02), S2 (0.03), C1 (0.03), N (0.00), C2 (0.01), C3 (−0.03); for complex B, Fe (−0.01), S1 (0.01), S2 (0.03), C1 (0.00), N (−0.01), C2 (0.02), C3 (−0.02). Similarly, interatomic distances and angles within the ligand conform to the corresponding values in related structures although the high thermal motion in the *n*-butyl group has resulted in very bad distances and angles for this group.

Magnetic Behavior. The magnetic nature of $(mebudtc)_3Fe$ polycrystallites has been studied between room temperature and liquid-nitrogen temperature in order to determined the high–low-spin thermal equilibrium of this complex. The main information was obtained through magnetic susceptibility temperature-dependent measurements and was further confirmed by Mössbauer spectroscopy. One advantage of the Mössbauer technique over the magnetic susceptibility is that it would allow observation of the two independent complexes

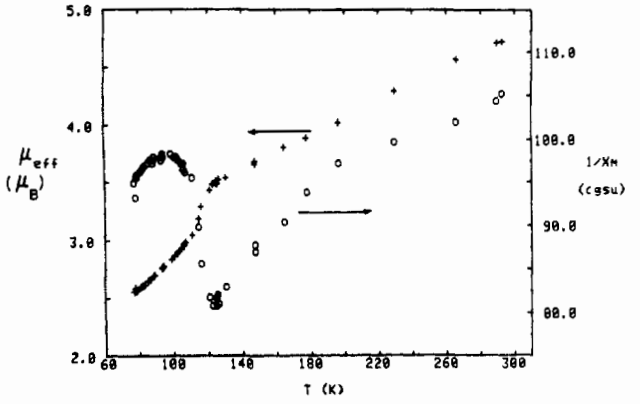

Figure 3. Plot of μ_{eff} and $1/\chi_M$ vs. temperature for $(mebudtc)_3Fe$.

A and B, provided the two iron(III) centers sense different electronic environments enough to induce variation in the ^{57}Fe quadrupole splitting (QS) and isomer shift (IS) of the two Mössbauer-active ions. Also, possible decomposition of $(mebudtc)_3Fe$ would become evident from the overall Mössbauer spectral pattern.[16] On the other hand, Mössbauer spectra alone cannot always provide conclusive proof for the spin state of ferric dithiocarbamato complexes.[5,21]

Effective Moment. The variation of the effective magnetic moment (μ_{eff}) of this complex in the temperature range between 300 and 77 K is shown in Figure 3 and indicates a drastic reduction of μ_{eff} as the temperature is lowered, typical of most ferric dtc complexes that exhibit high–low-spin equilibrium. At the high-temperature limit (μ_{eff}(300 K) = 4.7 μ_B) the spin $S = |^5/_2\rangle$ ground state is the predominant one, while at 77 K the majority of the molecules have crossed to the low-spin state (μ_{eff}(77 K) = 2.55 μ_B). However, since the crystal structure comprises equal numbers of each of the two independent and structurally different molecules A and B, the overall μ_{eff} measured here is the average of two $|^1/_2\rangle \rightleftarrows |^5/_2\rangle$ equilibrium rates corresponding to A and B. The apparent anomaly of the μ_{eff} or $1/\chi_M$ vs. T curve (Figure 3) at ca. 120 K may be attributed to either the combined high–low-spin equilibrium processes of complexes A and B or to the occurrence of a crystal phase transition. It should be mentioned here that $(dibudtc)_3Fe$ crystals exhibit a similar anomaly in the temperature dependence of their magnetic moment at about 130 K, which has been interpreted as an ordinary crystal phase transition.[3]

Comparison of the mean iron-sulfur distance ⟨Fe–S⟩ = 2.367 Å and μ_{eff} = 4.7 μ_B at 300 K with the corresponding values of other iron(III) tris(dithiocarbamato) complexes shows that these values fall well within the limits reported for other complexes and that there exists a general trend among these solids relating the increase in ⟨Fe–S⟩ length with increasing magnitude of μ_{eff} (Figure 1). The scattering of the points in Figure 3 probably reflects the fact that the ⟨Fe–S⟩ distance alone does not determine the strength of the ligand field, but the angular disposition of the iron–sulfur bonds also contributes to the field strength. Another possible cause for deviations from the above-mentioned trend, particularly with solvated complexes, can arise from the fact that solvent molecules are not permanently solvated at crystallographic sites of the lattice. Instead, they can readily escape even on standing under normal

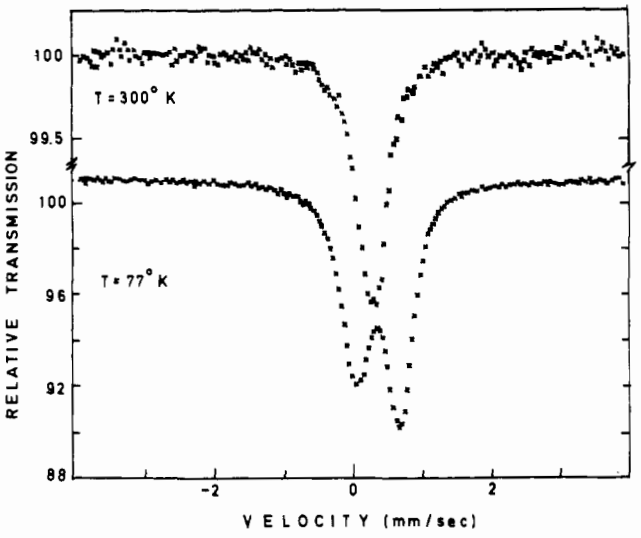

Figure 4. Mössbauer spectra of $(mebudtc)_3Fe$ at 300 and 77 K.

conditions, thus making the experimental value of μ_{eff} totally unreliable. Such unfortunate situations are known from the recent literature of the dtc complexes where authors were misled by magnetic measurements to assign intermediate ($S = |^3/_2\rangle$) ground spin states to some ferric tris(dithiocarbamato) complexes.[18] It was later shown however by combined Mössbauer and magnetic susceptibility studies that partial loss of solvated molecules was the cause of unreasonable μ_{eff} values.[16]

The conclusions drawn from magnetic susceptibility measurements are further corroborated by the Mössbauer spectra shown in Figure 4. The temperature dependence of the QS and its magnitude at low temperature are indicative of the prominent spin state.[20,21,27] In the present case the values of the QS, i.e. QS(300 K) = 0.1 mm/s and QS(77 K) = 0.61 mm/s, indicate a high-spin predominance at room temperature and a shift toward the low-spin configuration at 77 K, thus confirming the results of the magnetic susceptibility measurements. Isomer shift values, on the other hand, can only provide evidence for the spin state of iron(III) dtc complexes.[5,20,21] The measured IS in $(mebudtc)_3Fe$ at 300 and 77 K, which were found to be equal to 0.44 and 0.39 mm/s, respectively, follow the general trend expected for a predominantly high-spin ion at the high temperature and a shift toward low spin at lower temperature. Clearly the Mössbauer spectra of $(mebudtc)_3Fe$ are in very good agreement with the magnetic susceptibility measurements.

Another interesting parameter obtained from the low-temperature Mössbauer spectrum is the width of the absorption lines, which is quite larger (~0.5 mm/s) than the experimental width of the iron source (~0.29 mm/s). This may indicate that either there are two overlapping spectra with different IS and QS values corresponding to the two independent and structurally different complexes A and B or that the observed broadening is due to spin–lattice relaxation, which is known to predominate at this temperature. The latter explanation is further supported by the large asymmetry of the spectral pattern.

Registry No. $(mebudtc)_3Fe$, 36763-17-4.

Supplementary Material Available: Listings of hydrogen atom parameters, thermal parameters of non-hydrogen atoms, and observed and calculated structure factors and a stereoscopic view of the molecular packing at 300 K (10 pages). Ordering information is given on any current masthead page.

(21) Golding, R. M. *Mol. Phys.* **1967**, *12*, 13.
(22) Pound, R. V.; Rebka, G. A. *Phys. Rev. Lett.* **1960**, *4*, 274.
(23) Hoskins, B. F.; Kelly, B. P. *Chem. Commun.* **1968**, 1517.
(24) Albertson, J.; Oskarsson, A.; Stahl, K.; Svensson, C.; Ymen, I. *Acta Crystallogr. Sect. B: Struct. Crystallogr. Cryst. Chem.* **1981**, *B37*, 50.
(25) Albertsson, J.; Elding, I.; Oskarsson, A. *Acta Chim. Scand., Ser. A* **1979**, *A33*, 703.
(26) Albertsson, J.; Oskarsson, A. *Acta Crystallogr., Sect. B: Struct. Crystallogr. Cryst. Chem.* **1977**, *B55*, 1871.
(27) Mitra, S.; Raston, C. L.; White, A. H. *Aust. J. Chem.* **1976**, *29*, 1899.
(28) Bereman, R. D.; Churchill, M. R.; Nalewajek, D. *Inorg. Chem.* **1979**, *18*, 3112.